Supplementary Information

Stable anion radicals based on triazole-fused furazano[3,4-b]pyrazine scaffold

Daniil E. Efanov,[a] Svyatoslav E. Tolstikov,[a] Galina V. Romanenko,[a] Gleb A. Letyagin,[a] Kristina A. Smirnova,[a] Platon A. Chernavin,[a] Sergey L. Veber,[a] Nikolay F. Romashev,[b] Natalya A. Osik[a] and Artem S. Bogomyakov[a]

[a]FSBIS International Tomography Center of the Siberian Branch of the Russian Academy of Sciences, Institutskaya st., 3A.
[b]Nikolaev Institute of Inorganic Chemistry of the Siberian Branch of Russian Academy of Sciences, Acad. Lavrentiev Ave., 3.

Reagents and solvents

5,6-Dichlorofurazano[3,4-*b*]pyrazine was obtained according to the literature[1]. Phenylhydrazine (Aldrich, 97%) and pentafluorophenylhydrazine (Macklin, 98%), as well as solvents (ethylacetate (Chemical Line Co. Ltd, 99.5%), THF (JSC «Vekton», 99.95%), ethylene glycol (JSC «Baza №1 Khimreaktivov», >98%)) and triethylamine (Sigma Aldrich, 99%) were used without further purification. Chromatography grade silica gel (Silica 60, Macherey-Nagel GmbH & Co. KG) and alumina (AOK-63-21, JSC "Soyuzkhimprom") were used for cyclization procedures.

Synthetic procedures

6-phenyltriazolo[4,5-e]furazano[3,4-b]pyrazine, H_2L^{Ph}

An ice-cooled solution of phenylhydrazine (102 µl, 1.05 mmol) and triethylamine (146 µl, 1.05 mmol) in THF (3 ml) was stirred for 10 min. Then, a solution of 5,6-dichlorofurazano[3,4-*b*]pyrazine (100 mg, 0.52 mmol) in THF (1 ml) was added in one portion. After 1 hour at 0 °C mixture was evaporated, dissolved in EtOAc (15 ml) and extracted with H_2O (3x15 ml). Organic layer was separated, dried with Na_2SO_4 and evaporated until orange solid is formed (~98 % conversion by mass). This crude product was used in the cyclization protocols directly. As expected, it primarily consisted of **hyd(Ph)**, as shown by PXRD pattern (Figure S6).

Cyclization procedures:

With silica gel or aluminum oxide:

In a 10 ml round-bottom flask **hyd(Ph)** (40 mg, 0.12 mmol), EtOAc (2 ml) and silica gel (200 mg) were placed. Open flask was left with stirring (600 rpm) for 24 hours at room temperature. Then, suspension was filtered and washed with EtOAc and THF. Filtrate was kept on air, until most solvent evaporated (~3 days). Resulting crystals were filtered and washed with EtOAc. Product $\mathbf{H_2L^{Ph}}$ was collected as an olive-to-brown crystalline powder (19 %).

With high-temperature treatment:

In a 10 ml Erlenmeyer flask **hyd(Ph)** (40 mg, 0.12 mmol) and ethylene glycol (2 ml) were placed. Open flask was left with stirring (600 rpm) and heating of the stove set at 200 °C for 24 hours. Then, solution was cooled and diluted with water (8 ml), filtered, dried and washed with EtOAc and THF. Filtrate was kept on air, until most solvent evaporated (~3 days). Resulting crystals were filtered and washed with EtOAc. Product $\mathbf{H_2L^{Ph}}$ was collected as an olive-to-brown crystalline powder (17 %).

Structure confirmed by SCXRD[2]. Purity of the sample confirmed by PXRD (Figure S7). Elemental analysis, found (%): C, 49.51; H, 2.91; N, 40.45. Calculated (%): C, 49.79; H, 2.93; N, 40.65 ($C_{10}H_7N_7O$). NMR (DMSO-d_6, δ, ppm): ^{1}H: 11.08 (s, NH), 7.62 (d, *o*-H: $J_{H\text{-}H}$ = 8.6 Hz), 7.43 (t, *m*-H: $^1J_{H\text{-}H}$ = 7.5 Hz, $^2J_{H\text{-}H}$ = 8.6 Hz), 7.17 (t, *p*-H, $^1J_{H\text{-}H}$ = 7.5 Hz) (Figure S11); ^{13}C: 147.49, 139.47, 138.07, 129.52, 124.57, 115.30 (Figure S12). IR, ν/cm^{-1} (KBr tablet): 3268, 1597, 1576, 1498, 1477, 1374, 1317, 1006, 932, 828, 756, 689 (Figure S16).

6-pentafluorotriazolo[4,5-e]furazano[3,4-b]pyrazine, H_2L^F

An ice-cooled solution of pentafluorophenylhydrazine (208 mg, 1.05 mmol) and triethylamine (146 µl, 1.05 mmol) in THF (3 ml) was stirred for 10 min. Then, a solution of 5,6-dichlorofurazano[3,4-*b*]pyrazine (100 mg, 0.52 mmol) in THF (1 ml) was added in one portion. After 1 hour at 0 °C mixture was evaporated, dissolved in EtOAc (10 ml) and extracted with H_2O (3x15 ml). Organic layer was separated, dried with Na_2SO_4 and concentrated on a rotary evaporator at 50 °C. Orange intermediate was put through a chromatography column (SiO_2, C_7H_{16}-EtOAc gradient). Transparent crystals of $\mathbf{H_2L^F}$ grew from eluated fractions, which were washed with small amounts of CH_2Cl_2 to clean from the dark colored residue (42 %).

Pure sample was obtained by the following procedure. $\mathbf{H_2L^F}$ was suspended in distilled H_2O and boiled. Then EtOH was added dropwise until all substance was dissolved. Solution was cooled, whereupon white needles of $\mathbf{H_2L^F}$ would precipitate. They were filtered, dried, redissolved in EtOAc:C_7H_{16} (2:1) and left in a tall vial to slowly evaporate, leaving large crystals of pure $\mathbf{H_2L^F}$.

Structure confirmed by SCXRD (Table S2). Purity of the sample confirmed by PXRD (Figure S8). Elemental analysis, found (%): C, 36.36; H, 0.65; N, 29.70; F, 28.86. Calculated (%): C, 36.27; H, 0.61; N, 29.61; F, 28.68 ($C_{10}H_2F_5N_7O$). NMR (DMSO-d_6, δ, ppm): ^{1}H: 11.29 (s, NH) (Figure S13); ^{19}F: -148.79 (d, *o*-F, $^1J_{F\text{-}F}$ = 18.9 Hz), -155.81 (t, *p*-F, $^2J_{F\text{-}F}$ = 23.2 Hz), -161.71 (t, *m*-F, $^1J_{F\text{-}F}$ = 18.9 Hz, $^2J_{F\text{-}F}$ = 23.2 Hz) (Figure S14); ^{13}C: 147.22, 141.62, 139.97, 137.73, 116.01 (Figure S13); IR, ν/cm^{-1} (KBr tablet): 3175, 1604, 1587, 1529, 1483, 1316, 1268, 1089, 996, 916, 847, 827, 573 (Figure S15).

Tetrabutylammonium 6-phenyl[4,5-e]furazano[3,4-b]pyrazinide, $\mathbf{TBA^+L^{Ph\cdot-}}$

Mixture of $\mathbf{H_2L^{Ph}}$ (20 mg, 0.08 mmol), NaOH (35 mg, 0.88 mmol) and H_2O (10 ml) was stirred for 30 minutes. TBABr (103 mg, 0.32 mmol) was then added and mixture was further stirred for 3 hours at room temperature. Precipitate was filtered, dried and recrystallized from CH_2Cl_2:C_6H_{14} (3:1) at 4 ºC. Product is isolated as deep blue crystals (97 %).

Structure confirmed by SCXRD (Table S2). Purity of the sample confirmed by PXRD (Figure S9). Elemental analysis, found (%): C, 64.77; H, 8.13; N, 23.28. Calculated (%): C, 64.83; H, 8.58; N, 23.26 ($C_{26}H_{41}N_8O$). IR, ν/cm^{-1} (KBr tablet): 2962, 2932, 2874, 1589, 1556, 1515, 1487, 1462, 1415, 1394, 1179, 1013, 817, 752, 684, 613 (Figure S18). SQUID magnetometry study showed μ_{eff} values close to 1.73 μ_B, which corresponds to one unpaired electron per formula unit.

Tetrabutylammonium 6-pentafluorophenyl[4,5-e]furazano[3,4-b]pyrazinide, $\mathbf{TBA^+L^{F\cdot-}}$

Mixture of $\mathbf{H_2L^F}$ (30 mg, 0.09 mmol), NaOH (40 mg, 0.99 mmol) and H_2O (10 ml) was stirred for 2 hours. TBABr (116 mg, 0.36 mmol) was then added and mixture was further stirred for 24 hours at room temperature. Precipitate was filtered, dried and collected as deep green-blue powder (84 %).

Pure sample was obtained by the following procedure. $\mathbf{TBA^+L^{F\cdot-}}$ was suspended in distilled H_2O and boiled. Then EtOH was added dropwise until most of the substance was dissolved. Hot solution was filtered, filtrate was concentrated by boiling and left to cool, which led to precipitation of thin black needles of $\mathbf{TBA^+L^{F\cdot-}}$, which were filtered, dried and collected.

Structure confirmed by SCXRD (Table S2). Purity of the sample confirmed by PXRD (Figure S10). Elemental analysis, found (%): C, 54.21; H, 6.22; N, 19.40; F, 16.63. Calculated (%): C, 54.63; H, 6.35; N, 19.60; F, 16.62 ($C_{26}H_{36}F_5N_8O$). IR, ν/cm^{-1} (KBr tablet): 2965, 2878, 1530, 1517, 1395, 1185, 1090, 994, 952, 830 (Figure S19). SQUID magnetometry study showed μ_{eff} values close to 1.73 μ_B, which corresponds to one unpaired electron per formula unit.

Electron paramagnetic resonance (EPR) spectroscopy

EPR measurements were performed using commercial Bruker EMX X-band EPR spectrometer. The samples consisted of solutions of the studied radicals in EtOH:H_2O (1:1) with concentration of 10^{-3} M, placed in glass sample tubes (outer diameter = 1.6 mm). Continuous wave (CW) EPR spectra were recorded at conditions that avoided unwanted modulation broadening and microwave saturation.

Simulation of the CW EPR spectra were carried out using the EasySpin (6.0.0) software package[3]. Final iteration of fitting programs for $\mathbf{L^{Ph\cdot-}}$ and $\mathbf{L^{F\cdot-}}$ are given:

```
clear, clf

[field,sign] = eprload('DE5_10m3Conc_6Best24dB81Scans');

Exp.mwFreq = 9.87377;
Exp.Range = [347.5,355.5];
Exp.nPoints = 2048;

Sys.g = [2.0090] ;
Sys.Nucs = '14N, 14N, 14N, 14N, 1H, 1H, 1H';
Sys.n = [2 2 2 1 2 2 1]
Sys.A = [4.98 9.10 0.48 14.29 -4.86 1.85 -5.38];
Sys.lwpp = [0.0497, 0.0531];

[xa,ya] = garlic(Sys,Exp);
plot(xa,ya/max(ya),'b',field/10,sign/max(sign),'r');
ylim([-1.2 1.2])
xlim([347.5,355.5])
xlabel('magnetic field [mT]');

Vary.A = ([1.5 1.5 0.5 3.0 1.5 0.5 1.5]);
esfit(sign, @garlic, {Sys,Exp}, {Vary});
```

```
clear, clf

[field,sign] = eprload('DE158_10m3Conc_1Best24dB50Scans');

Exp.mwFreq = 9.87359;
Exp.Range = [347.5,355.5];
Exp.nPoints = 2048;

Sys.g = 2.0093;
Sys.Nucs = '14N, 14N, 14N, 14N, 19F, 19F, 19F' ;
Sys.n = [2 2 2 1 2 2 1];
Sys.A = [5.402, 11.660, 0.977, 11.563, 5.624, -1.728, 10.911];
Sys.lwpp = [0.0540, 0.0228];

[xa,ya] = garlic(Sys,Exp);
plot(xa,ya/max(ya),'b',field/10,sign/max(sign),'r');
ylim([-1.2 1.2])
xlim([347.5,355.5])
xlabel('magnetic field [mT]');

Vary.A = [0.0, 1.0, 0.2, 4.0, 1.0, 0.0, 1.0];
esfit(sign, @garlic, {Sys,Exp}, {Vary});
```

Computational methods

Quantum chemical calculations were performed with the ORCA program package (version 6.0.0.)[4]. The TPSSH/ma-def2-QZVPP method[5–7] with the Grimme dispersion correction D3BJ[8] accounting for the solvent (water) via the conductor-like polarizable continuum model (C-PCM)[9] was used to optimize the geometries of $\mathbf{L^{Ph\cdot-}}$ and $\mathbf{L^{F\cdot-}}$ as well as to calculate their hyperfine coupling constants and g-factors.

Cyclic voltammetry (CV)

The cyclic voltammograms (CV) of compounds $\mathbf{H_2L^{Ph}}$ and $\mathbf{H_2L^{F}}$ were recorded with a 797 VA Computrace system (Metrohm, Switzerland). All measurements were performed with a conventional three-electrode configuration consisting of glassy carbon working and platinum auxiliary electrodes and an Ag/AgCl/KCl reference electrode (V = 10 mL). The solvent used in all experiments was acetonitrile which was deoxygenated before use. Tetra-n-butylammonium hexafluorophosphate (0.1 M solution) was used as a supporting electrolyte. The concentration of $\mathbf{H_2L^{Ph}}$ and $\mathbf{H_2L^{F}}$ was 10^{-3} M. $E_{1/2}$ was calculated as the half-sum of the potentials of the anodic and cathodic peaks. The registered value of $E_{1/2}$ for the Fc^+/Fc couple was 0.43 V in acetonitrile.

Table S1. Table of half wave potentials or anode potentials and delta of two peaks

Compound	$E_{1/2}$ or E_a, V, (vs. Ag/AgCl) (ΔE, mV)
H_2L^{Ph}	$E_a = 0.88$
H_2L^{F}	$E_a = 1.18$
$\mathbf{L^{Ph2-}}$	$E_{1/2} = 0.18$ (73)
$\mathbf{L^{F2-}}$	$E_{1/2} = 0.35$ (98)

Magnetic measurements

The magnetic susceptibility of the polycrystalline samples was measured with a Quantum Design MPMS-XL SQUID magnetometer in the temperature range 2-300 K with magnetic field up to 5 kOe. Diamagnetic corrections were made using the Pascal constants[10]. The effective magnetic moment was calculated as $\mu_{eff}(T) = [(3k/N_A\mu_B^2)\chi T]^{1/2} \approx (8\chi T)^{1/2}/\mu_B$.

Single-crystal X-Ray diffraction (SCXRD)

SCXRD experiments were performed on AXS Smart Apex II (Bruker AXS, Mo-Kα radiation, λ = 0.71073 Å) diffractometer. A single crystal of each compound was covered with a layer of mineral oil and mounted on a Cryoloop™ for data collection. Data were collected using Apex2 program package[11] and the intensity data were corrected for absorption using multi-scan techniques (SADABS program, version 2.10)[12]. The structures were solved by direct methods and refined on F^2 by full-matrix least squares in an anisotropic approximation for non-hydrogen atoms. Hydrogen atoms were placed at calculated positions and refined using a riding model. All calculations were performed with the SHELX programs[13,14]. The crystallographic data and details of experiments are presented in Table S2. Selected bond lengths and angles are listed in Table S3. The crystallographic data were deposited at the Cambridge Crystallographic Data Centre and can be obtained free of charge at http://www.ccdc.cam.ac.uk/conts/retrieving.html (or from the CCDC, 12 Union Road, Cambridge CB2 1EZ, UK; Fax: +44 1223 336033; E-mail: deposit@ccdc.cam.ac.uk). Deposition Number(s): 2403749–2403751.

Table S2. Crystallographic Data and Experimental Details

Compound	H_2L^F	TBA^+L^{Ph-}	TBA^+L^{F-}
Formula	$C_{10}H_2F_5N_7O$	$C_{26}H_{41}N_8O$	$C_{26}H_{36}F_5N_8O$
FW	331.19	481.67	571.63
T, K	295	295	295
Space group, *Z*	*Cc,* 4	$P2_1/n$, 4	$P2_1/n$, 4
a, *b*, *c*, Å	6.2914(17) 28.492(7) 7.258(2)	8.5924(4) 17.8690(7) 18.4283(8)	10.4306(6) 20.1188(12) 14.4748(9)
α, *β*, *γ*, °	90 114.975(16) 90	90 92.076(3) 90	90 99.556(4) 90
V, Å^3	1179.3(6)	2827.6(2)	2995.4(3)
D_c, g cm^{-3}	1.865	1.132	1.268
θ_{max}, deg.	28.428	25.999	23.255
I_{hkl} (meas/uniq), R_{int}	5120 / 2333 0.0525	22641 / 5550 0.0365	21301 / 4305 0.0694
I_{hkl} ($I>2\sigma_I$) / Ns	995 / 209	2283 / 310	1504 / 371
GooF	0.738	0.948	0.999
R_1 / wR_2 ($I>2\sigma_I$)	0.0370 / 0.0383	0.0548 / 0.1654	0.0773 / 0.2248
R_1 / wR_2 (all data)	0.1310 / 0.0514	0.1514 / 0.2326	0.2075 / 0.3094
CCDC	2403749	2403750	2403751

Table S3. Selected bond lengths (Å) and angles (°) for studied compounds.

Compound	H_2L^{Ph}*	H_2L^{F}	$TBA^+L^{Ph\cdot-}$	$TBA^+L^{F\cdot-}$
N–O	1.3998(18) 1.4003(17)	1.399(5) 1.412(6)	1.404(3) 1.410(3)	1.388(7) 1.432(7)
$(C–N)_{Fur}$	1.290(2) 1.2955(19)	1.288(7) 1.307(6)	1.313(3) 1.314(3)	1.321(8)
$(C–C)_{Fur}$	1.4351(19)	1.421(8)	1.444(3)	1.462(9)
$C_{Fur}–N_{Pyr}$	1.3619(19) 1.3722(18)	1.359(6) 1.373(7)	1.348(3) 1.351(3)	1.330(8) 1.343(8)
$C_{Triaz}–N_{Pyr}$	1.3801(18) 1.3814(17)	1.371(6) 1.398(7)	1.336(3) 1.341(3)	1.342(7) 1.366(7)
$(C–N)_{Triaz}$	1.3085(19) 1.3118(17)	1.316(6) 1.325(6)	1.333(3) 1.340(3)	1.338(7) 1.346(7)
$(N–N)_{Triaz}$	1.3562(16) 1.3577(16)	1.358(6) 1.359(6)	1.344(2) 1.358(2)	1.325(6) 1.351(6)
$(C–C)_{Triaz}$	1.4068(18)	1.380(7)	1.431(3)	1.435(7)
$\angle(C–N–C)_{Pyr}$	114.61(12) 114.85(12)	114.6(5) 114.8(5)	108.6(2) 108.7(2)	108.6(6) 110.0(6)
$\angle(C_4N_7O, Ph)$	1.7	46.2	7.8	69.1

* see [Tolstikov, S. E.; Efanov, D. E.; Romanenko, G. V.; Egorov, M. P.; Ovcharenko, V. I. Structures of Reaction Products of 5,6-Dichlorofurazano[3,4-b]Pyrazine with R-Hydrazines. Russ. Chem. Bull. 2022, 71 (8), 1821–1825. https://doi.org/10.1007/s11172-022-3595-y].

a)

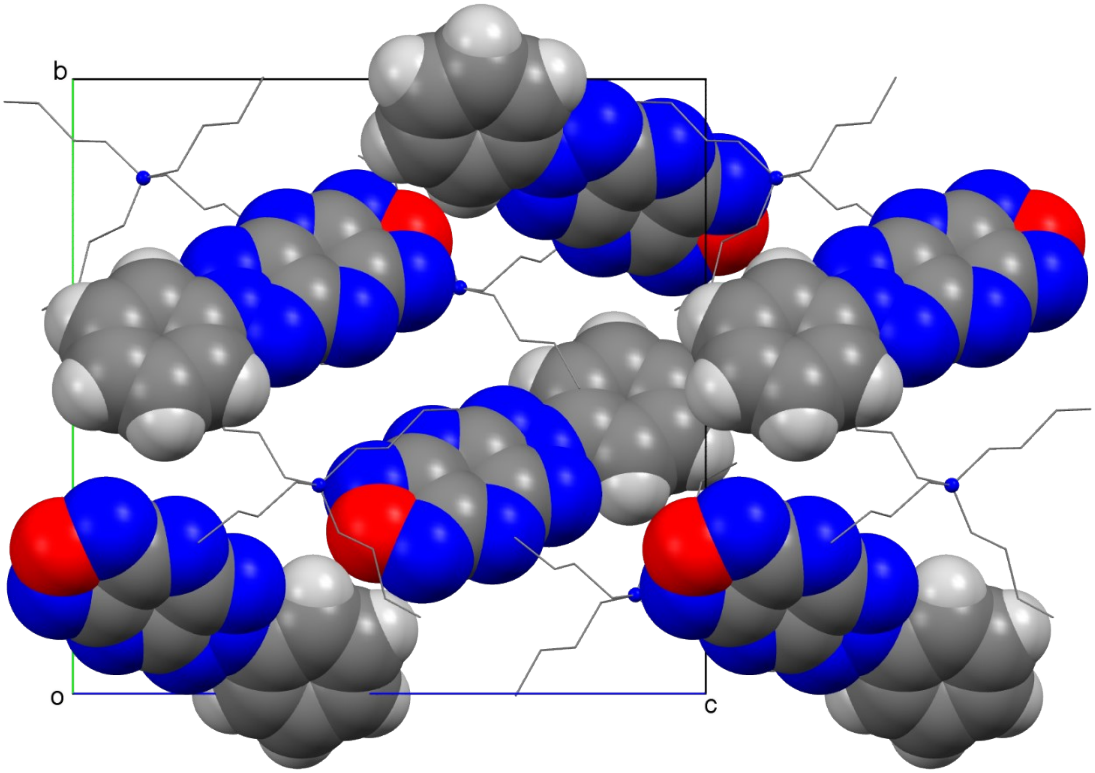

b)

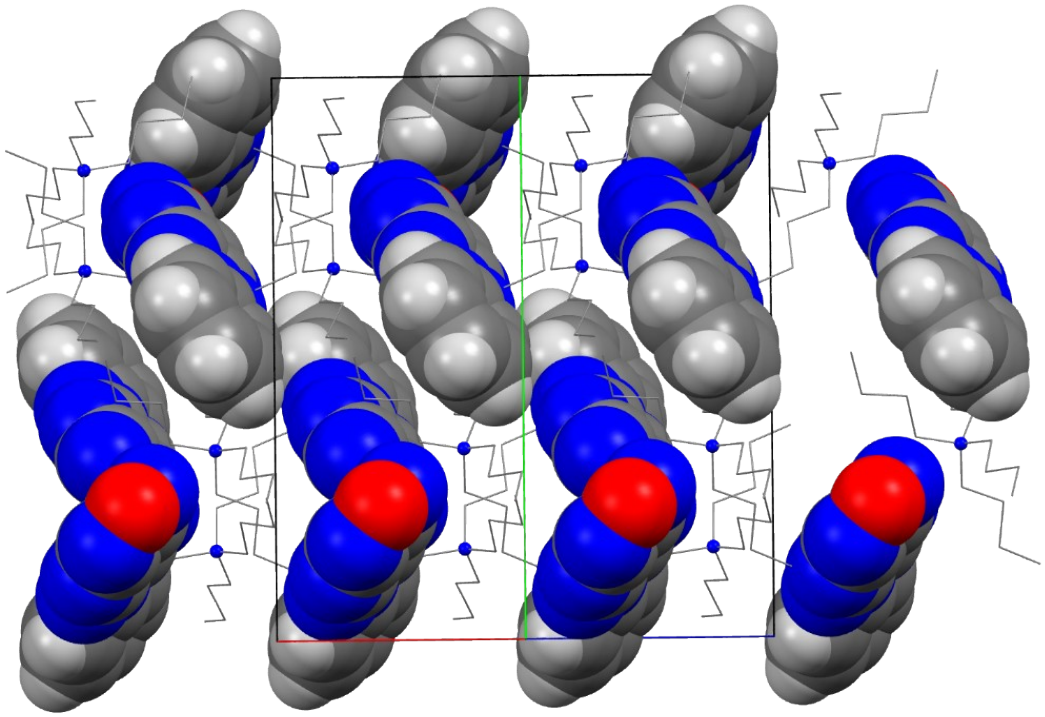

Figure S1. Packing of ions in the crystal structure of $\mathbf{L}^{\mathbf{Ph}\cdot-}$ viewed along [100] (a) and [101] (*b*).

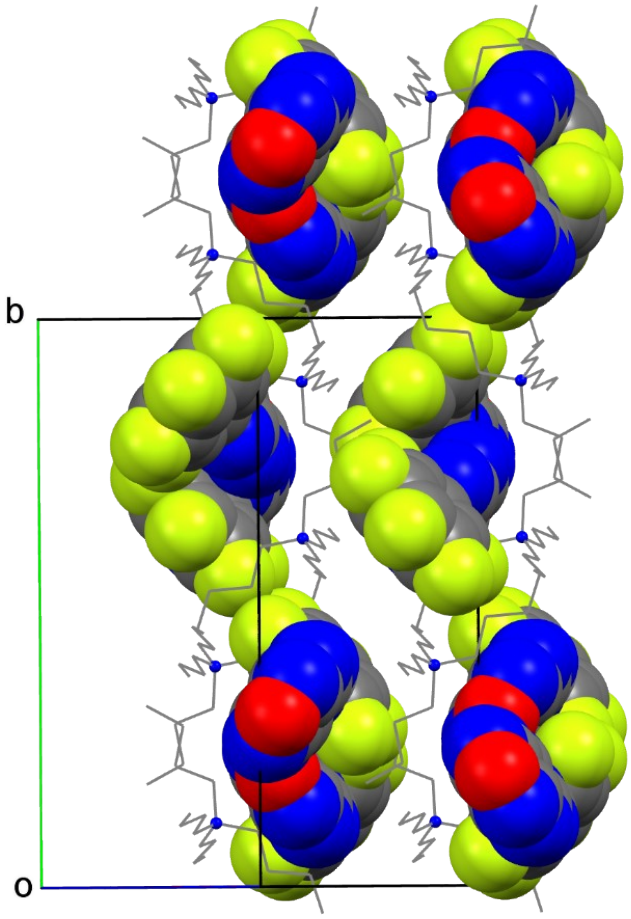

Figure S2. Packing of ions in the crystal structure of $\mathbf{L}^{F-}$ viewed along [1,0,-1].

Powder X-Ray diffraction (PXRD)

PXRD data were collected on a PowDix 600 (ADANI) diffractometer equipped with a MYTHEN2 R 1D (Dectris) detector at room temperature using CuKα radiation at a scanning speed on θ of 0.01°/s. The experimental patterns were compared to the simulated ones based on the crystal structures obtained by single crystal XRD. The clear match of peak positions between both experimental and simulated patterns indicates good crystal purity of the samples (SI).

Figure S3. PXRD pattern of crude **hyd(Ph)**

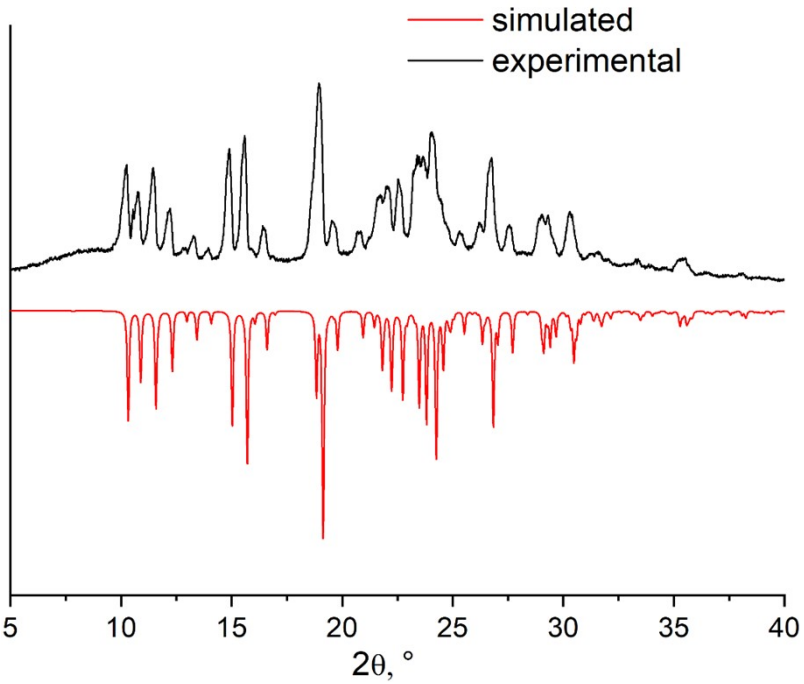

Figure S4. PXRD pattern of $\mathbf{H_2L^{Ph}}$

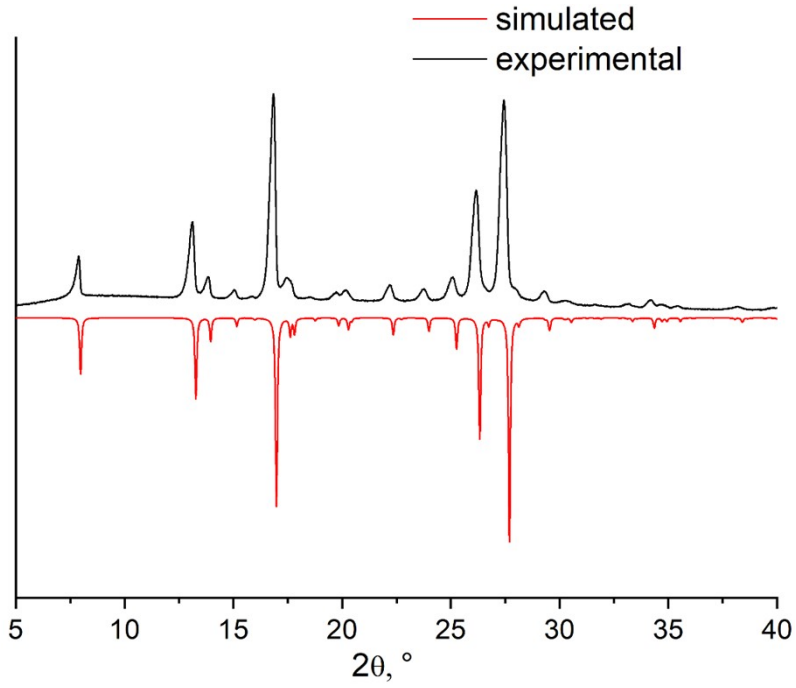

Figure S5. PXRD pattern of $\mathbf{H_2L^F}$

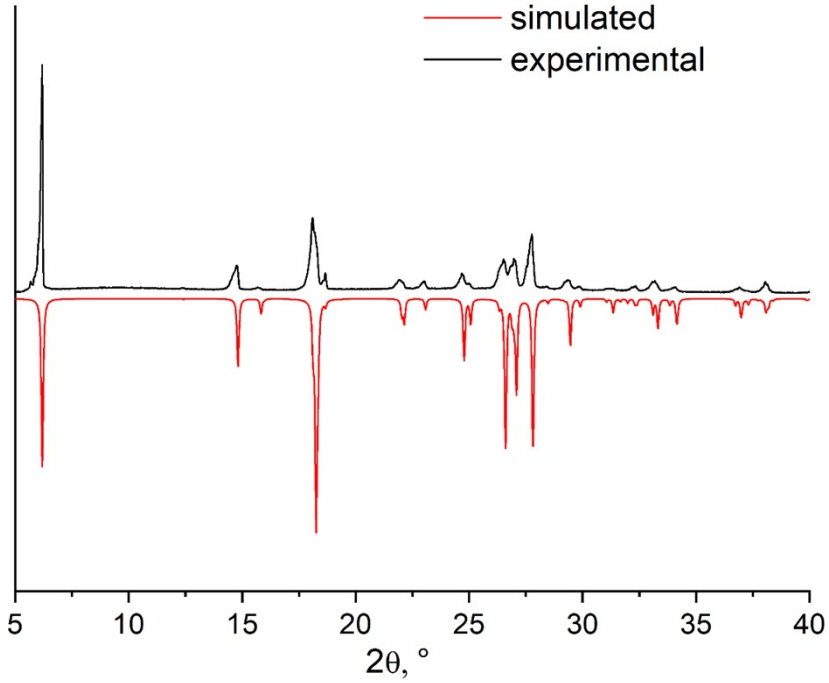

Figure S6. PXRD pattern of $\mathbf{TBA^+L^{Ph-}}$

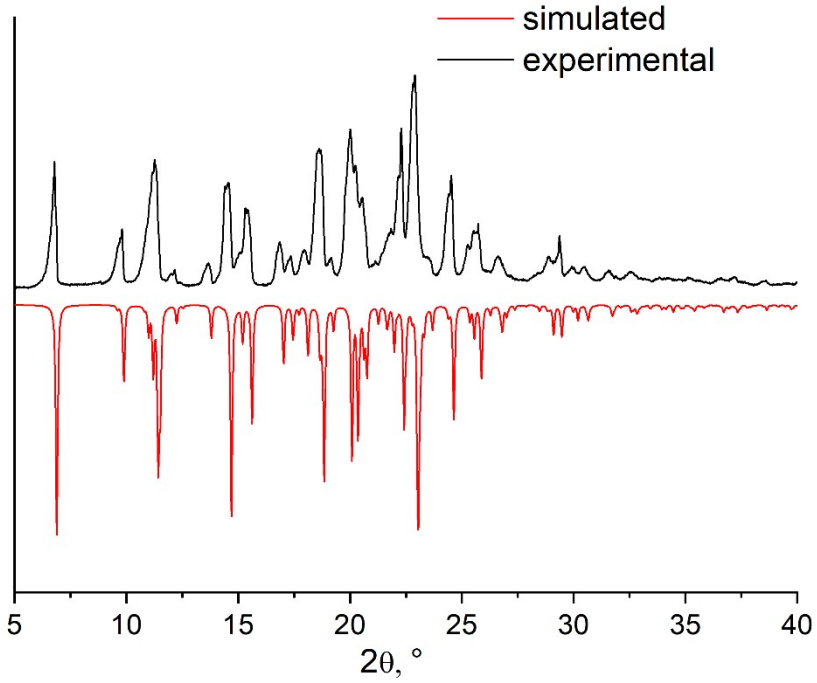

Figure S7. PXRD pattern of **TBA^{+}L^{F-}**

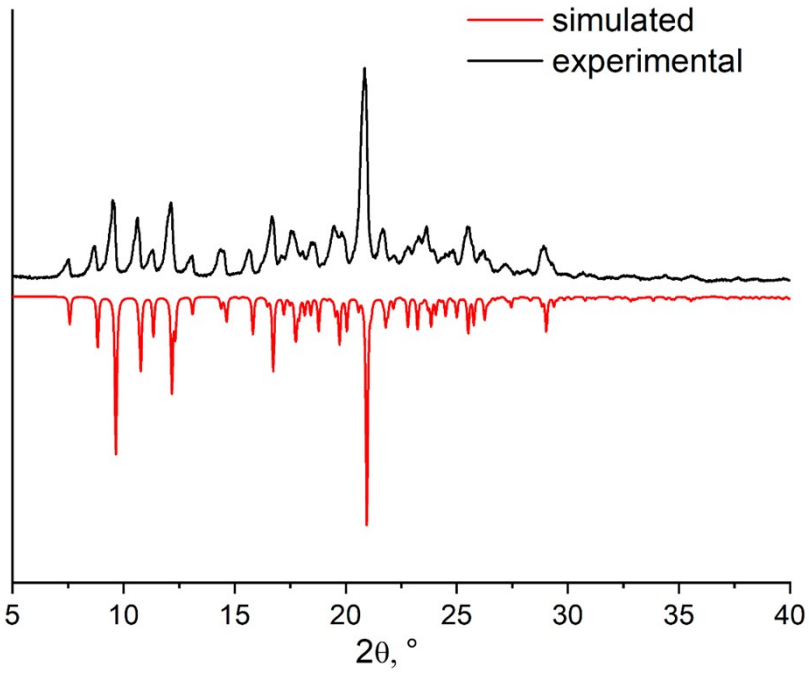

Nuclear magnetic resonance (NMR)

Figure S8. ^{1}H NMR spectra of $\mathbf{H_2L^{Ph}}$

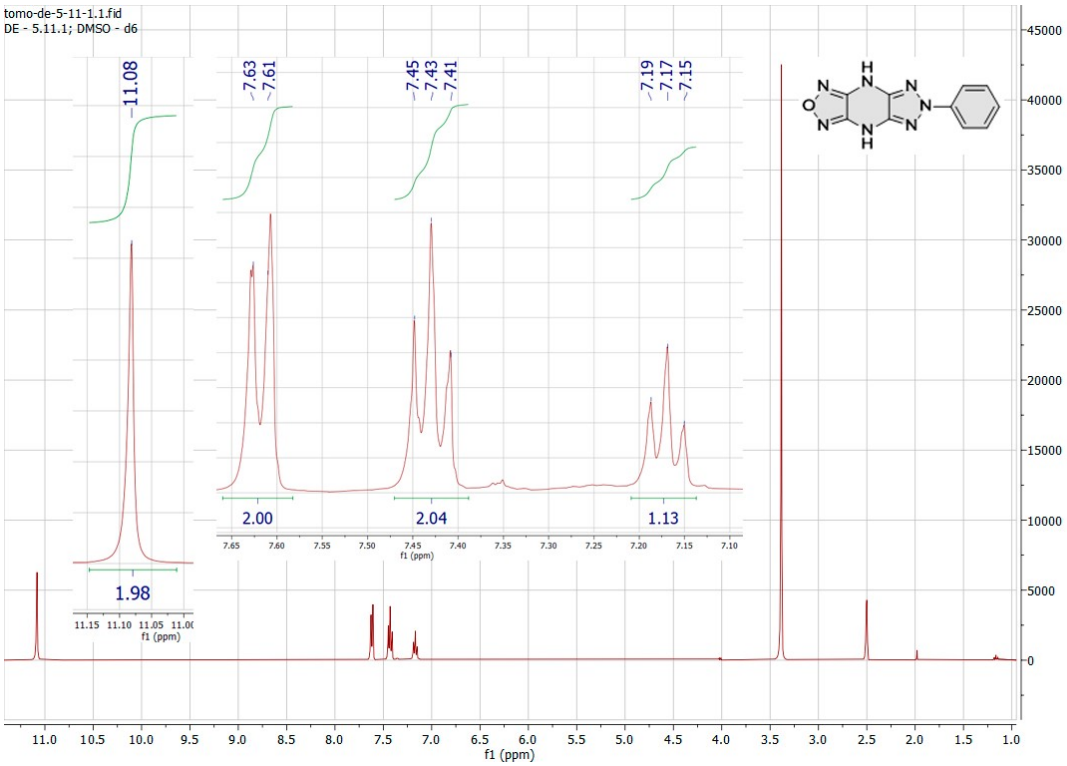

Figure S9. ^{13}C NMR spectra of $\mathbf{H_2L^{Ph}}$

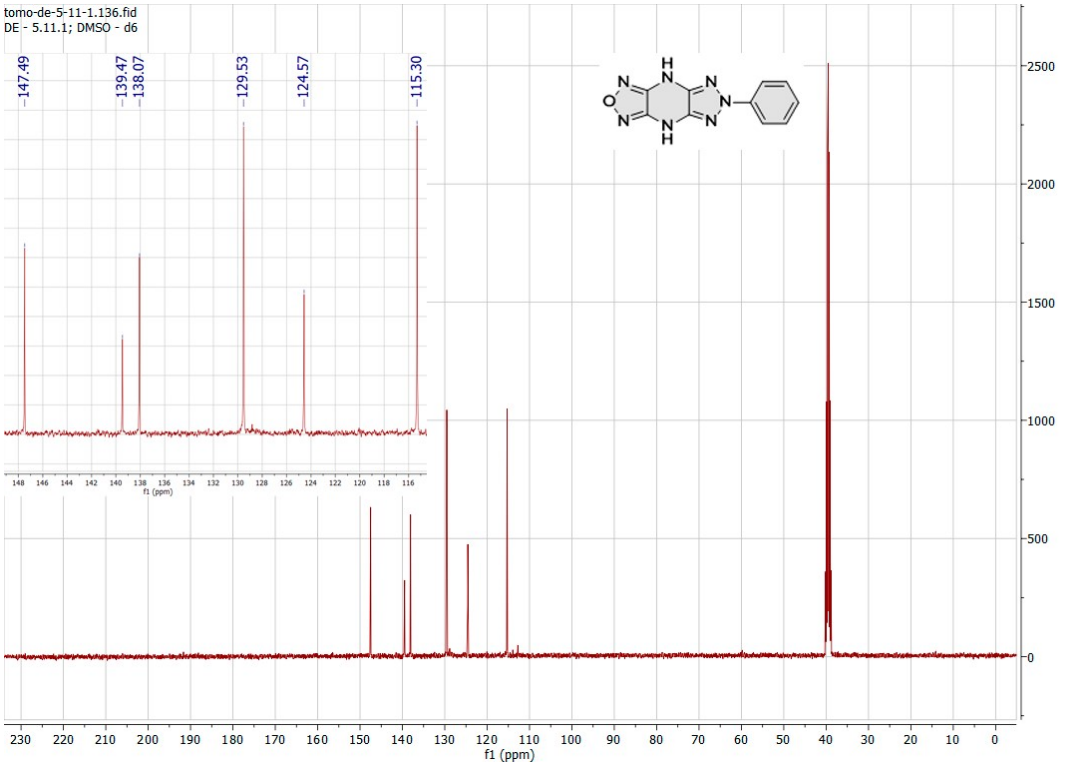

Figure S10. ^{1}H NMR spectra of $\mathbf{H_2L^F}$

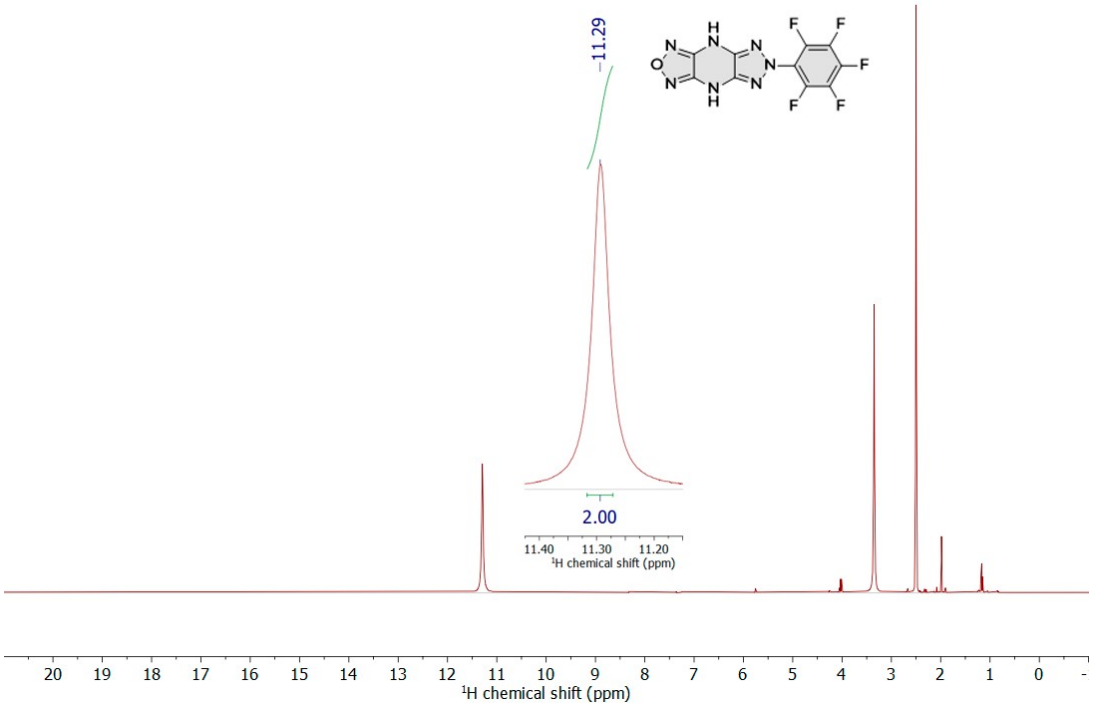

Figure S11. ^{19}F NMR spectra of $\mathbf{H_2L^F}$

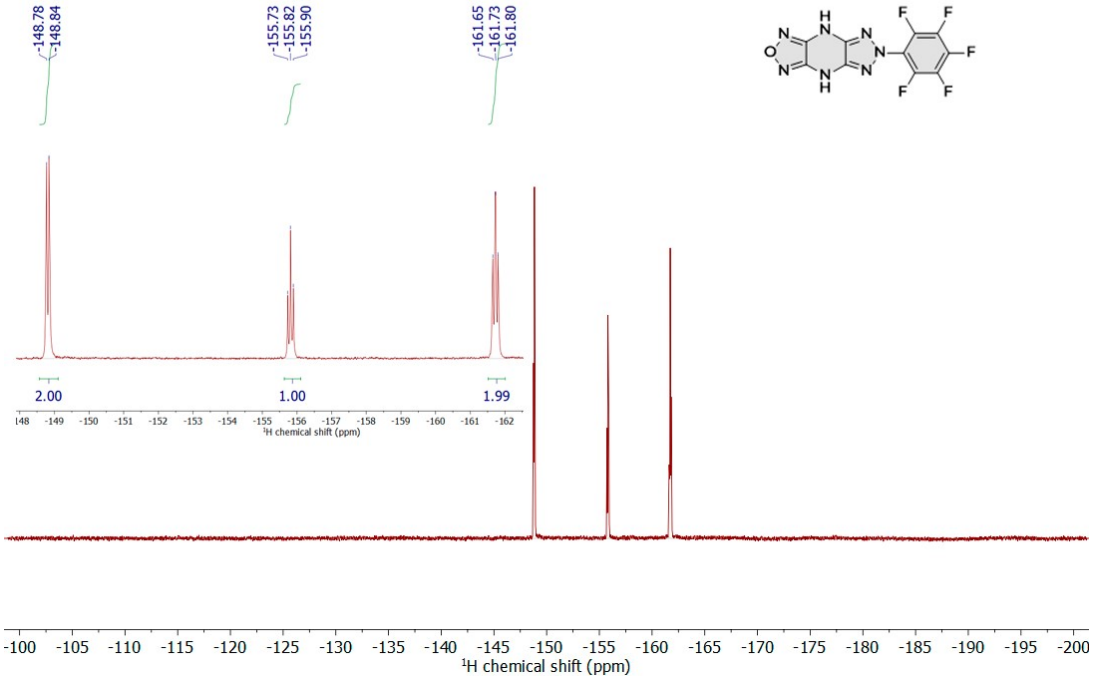

Figure S12. ^{13}C NMR spectra of $\mathbf{H_2L^F}$

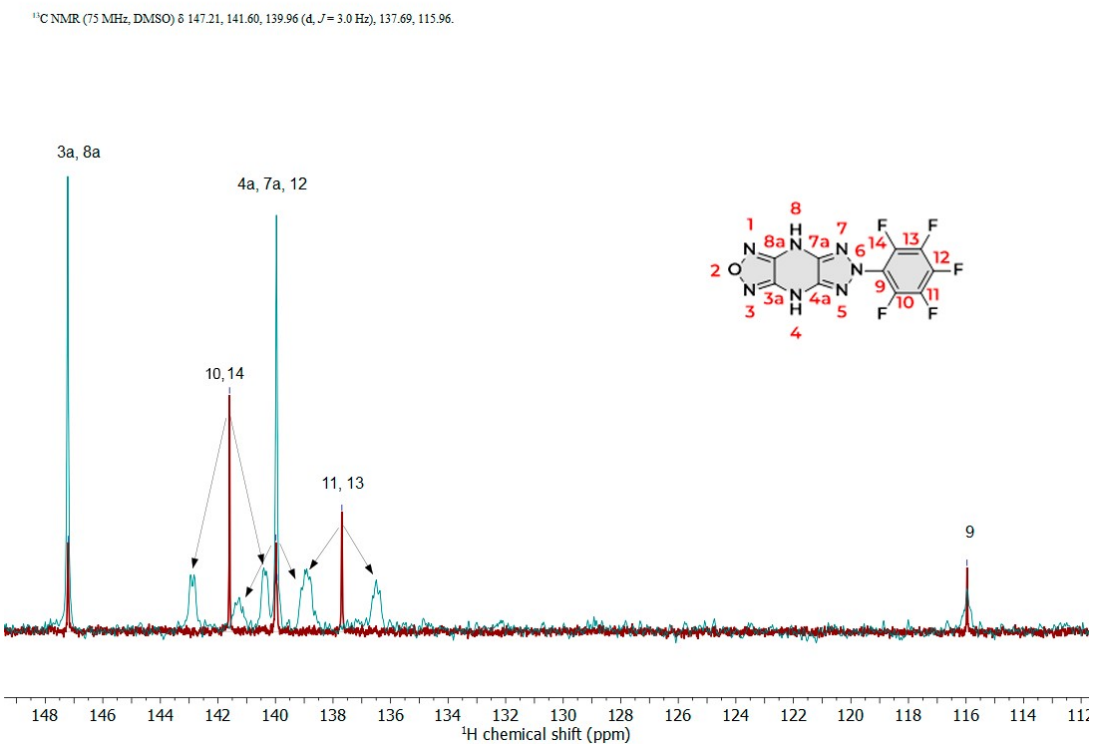

Note: ^{13}C NMR spectra of $\mathbf{H_2L^F}$ is comprised of two separately taken spectra: one with ^{19}F-decoupling (red), and the other – with ^{1}H-decoupling (blue). Obviously, coinciding peaks from both spectra correspond to ^{13}C nuclei, that are far from both ^{1}H and ^{19}F (3a, 4a, 7a and 8a). Peak, corresponding to nucleus 9 has a second-order coupling constant with ^{19}F and is only slightly splitted when ^{1}H-decoupling is on. Peaks of nuclei 10, 11, 13 and 14 are split considerably when ^{1}H-decoupling is on, and collapse back to a singlet when ^{19}F-decoupling is on. Coincidentally, peak of nucleus 12 is located at the same ppm as 4a and 7a, so it splits without ^{19}F-decoupling as well.

Infrared spectroscopy (IR)

Figure S13. IR spectra of $\mathbf{H_2L^{Ph}}$

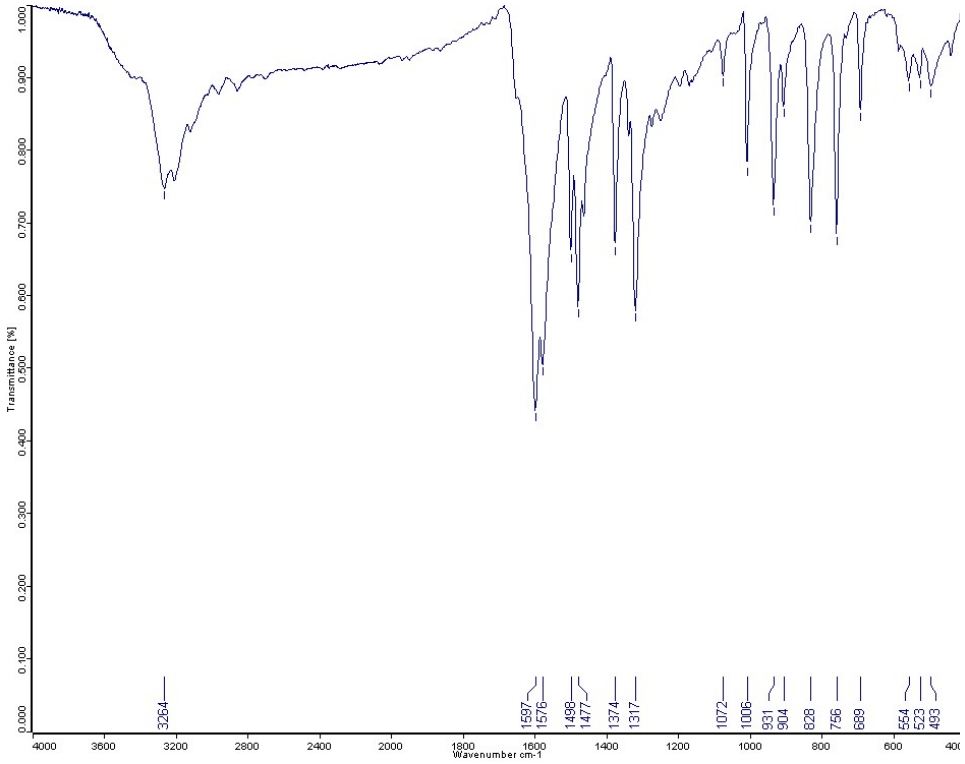

Figure S14. IR spectra of $\mathbf{H_2L^{F}}$

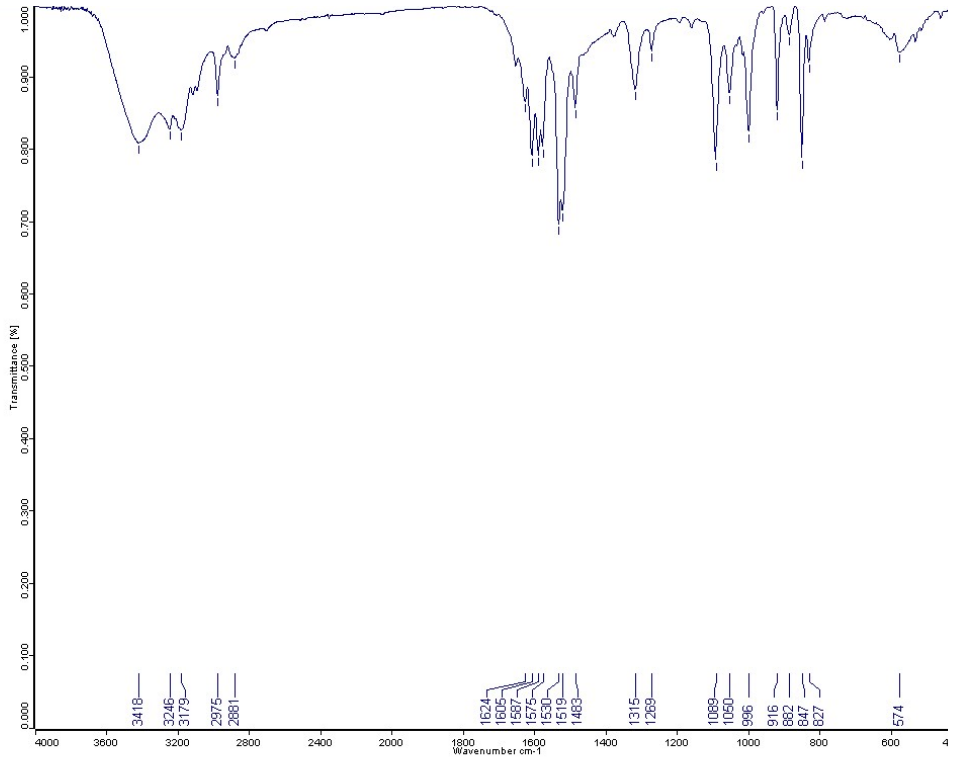

Figure S15. IR spectra of **TBA^{+}L^{Ph-}**

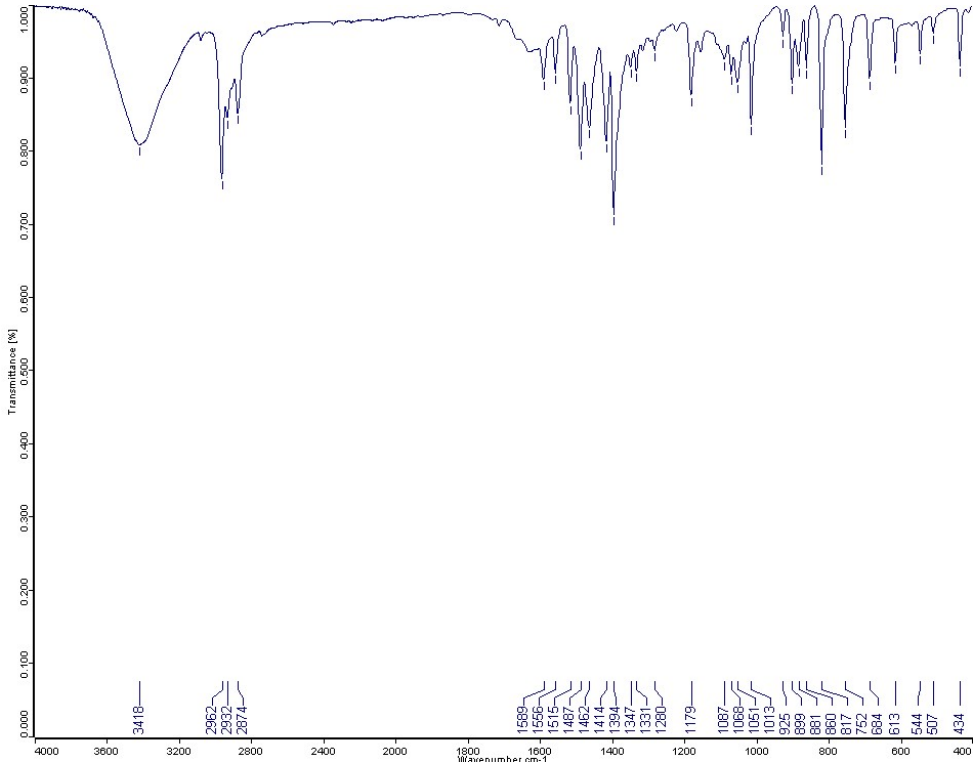

Figure S16. IR spectra of **TBA^{+}L^{F-}**

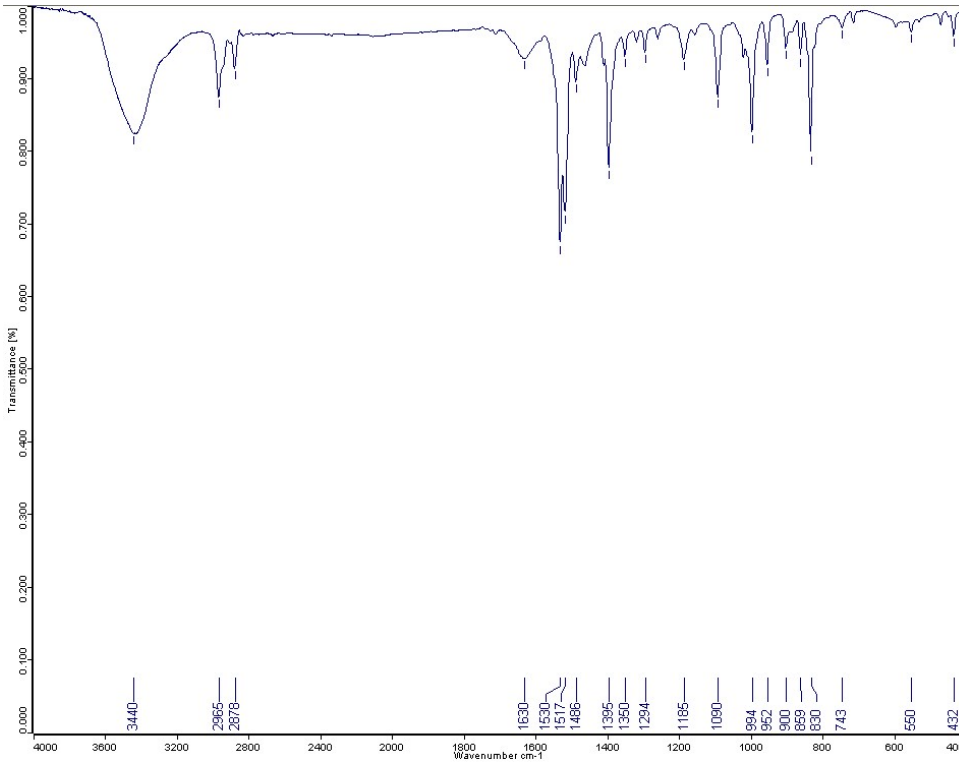

Optical properties

Steady-state UV–visible absorption spectra were recorded using an Agilent 8453 spectrophotometer from Hewlett-Packard (La Jolla, CA, USA). Fluorescence measurements were performed with an FLSP920 spectrofluorometer (Edinburg Instruments, Edinburg, Great Britain). All measurements were carried out in a 10×10 mm^2 quartz cell.

Figure S17. excitation band (black) and emission band (red) of coumarin 153.

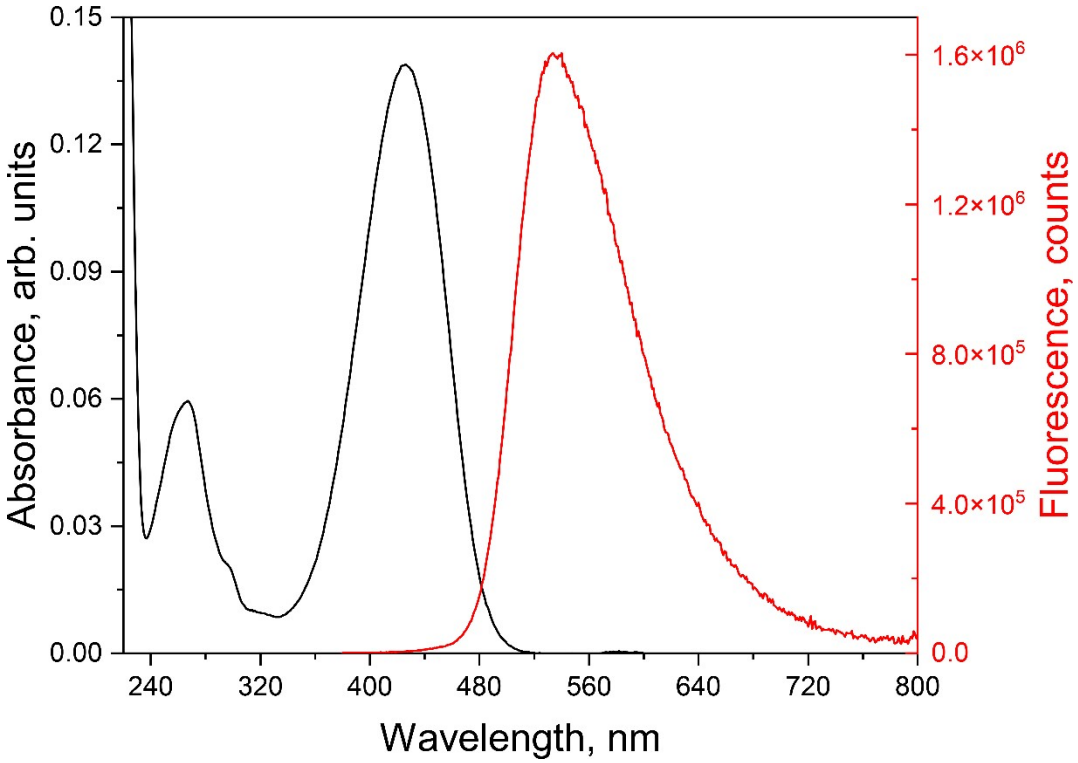

1 E. S. Childress, J. M. Salamoun, S. R. Hargett, S. J. Alexopoulos, S.-Y. Chen, D. P. Shah, J. Santiago-Rivera, C. J. Garcia, Y. Dai, S. P. Tucker, K. L. Hoehn and W. L. Santos, *J. Med. Chem.*, 2020, **63**, 2511–2526.
2 S. E. Tolstikov, D. E. Efanov, G. V. Romanenko, M. P. Egorov and V. I. Ovcharenko, *Russ Chem Bull*, 2022, **71**, 1821–1825.
3 S. Stoll and A. Schweiger, *Journal of Magnetic Resonance*, 2006, **178**, 42–55.
4 F. Neese, F. Wennmohs, U. Becker and C. Riplinger, *The Journal of Chemical Physics*, 2020, **152**, 224108.
5 Minimally augmented Karlsruhe basis sets | Theoretical Chemistry Accounts, https://link.springer.com/article/10.1007/s00214-010-0846-z, (accessed October 2, 2024).
6 F. Weigend and R. Ahlrichs, *Phys. Chem. Chem. Phys.*, 2005, **7**, 3297–3305.
7 V. N. Staroverov, G. E. Scuseria, J. Tao and J. P. Perdew, *The Journal of Chemical Physics*, 2003, **119**, 12129–12137.
8 A. D. Becke, *The Journal of Chemical Physics*, 1992, **96**, 2155–2160.
9 Fast Evaluation of Geometries and Properties of Excited Molecules in Solution: A Tamm-Dancoff Model with Application to 4-Dimethylaminobenzonitrile | The Journal of Physical Chemistry A, https://pubs.acs.org/doi/10.1021/jp000156l, (accessed October 2, 2024).
10 Diamagnetic Corrections and Pascal's Constants | Journal of Chemical Education, https://pubs.acs.org/doi/abs/10.1021/ed085p532, (accessed October 2, 2024).
11 Bruker, APEX2, SAINT-Plus and XPREP Bruker AXS Inc., Madison (USA) 2004.
12 L. Krause, R. Herbst-Irmer, G. M. Sheldrick and D. Stalke, *J Appl Cryst*, 2015, **48**, 3–10.
13 (IUCr) SHELXT – Integrated space-group and crystal-structure determination, https://journals.iucr.org/a/issues/2015/01/00/sc5086/index.html, (accessed October 29, 2024).
14 G. M. Sheldrick, *Acta Cryst C*, 2015, **71**, 3–8.